

Synthesis of Hydroxyapatite-Polyethylene Glycol with *In-Situ* Method Using Calcium Oxide from Blood Shells (*Anadara granosa*)

Novesar Jamarun^{1*}, Nabila Ayyu Trycahyani¹, Syukri Arief¹, Upita Septiani¹, and Vivi Sisca²

¹Department of Chemistry, Andalas University, Limau Manis, Padang 25163, Indonesia

²Department of Biology Education, Institute of Education YPM Bangko, Jl. Jenderal Sudirman, Meranging, Jambi 37313, Indonesia

* **Corresponding author:**

email: novesarjamarun@sci.unand.ac.id

Received: October 21, 2022

Accepted: January 23, 2023

DOI: 10.22146/ijc.78538

Abstract: Hydroxyapatite ($\text{Ca}_{10}(\text{PO}_4)_6(\text{OH})_2$, HAp) is a calcium phosphate-based biomaterial that is widely used in bone implants due to its similarity in composition with the constituent elements of bone. However, HAp still has poor mechanical properties, so research was carried out to improve the mechanical properties such as reduced brittleness, less fracture resistance, and a denser structure of HAp by synthesizing composites with PEG. This study used PEG as a filler and HAp as a matrix. HAp was synthesized from blood clam shells (*Anadara granosa*) using the sol-gel method. HAp-PEG composite was synthesized using the in-situ method with various HAp concentrations of 40, 50, 60, 70, and 80%. FTIR characterization showed the presence of functional groups PO_4^{3-} and CO_3^{3-} , which indicated the presence of HAp. Analysis of the XRD pattern showed a crystal size of 24.194 nm. SEM-EDX showed the needle-shaped HAp-PEG composite HAp crystal morphology and obtained a Ca/P ratio of 1.87. Analysis of DTA results showed a weight loss of 65.72% in the composite at a temperature > 200 °C. A degradation test was also carried out to see the percentage of the HAp-PEG composite to be degraded, and the optimum degraded composite with increasing days had a concentration of 70%.

Keywords: hydroxyapatite; HAp-PEG composite; in-situ method; blood shells

■ INTRODUCTION

According to the Pharmaceutical and Medical Technology Center (PTFM), BPPT needs around 120,000 bones each year with a value of around Rp 600 billion. Based on data from the statistics center in 2018, bone implants needed in Indonesia are around Rp 27 trillion, and this data has continued to increase since 2016. This report shows that Indonesia's need for bone implants is very high. As a complex system and the most important constituent part of the human body, which consists of hydroxyapatite (HAp) and type 1 collagen fibrils (70% HAp, 20% collagen, and 10% water), if there is damage to the bone, it needs to be repaired [1-2].

One way to overcome this problem is to use bone graft material to replace bone. One of the requirements for the replacement material in human bones is that it is biocompatible. It does not cause a rejection reaction from

the human immune system because it is considered a foreign object [2-3]. Bioceramic material that is often used in biomedical applications is synthetic HAp, $\text{Ca}_{10}(\text{PO}_4)_6(\text{OH})_2$, as bone graft material [3]. Due to the similarity of composition and mineral phase in bone, having excellent biocompatibility, ability to assist cell function, and osteoconductivity, HAp is used as one of the alternative materials for bone graft material [4].

HAp is a bioceramic material with strong chemical bonds, bioactive with high bioaffinity [5-6]. Calcium phosphate is the main constituent of HAp, also contained in bone. HAp, as a biomaterial, can be synthesized from various sources, including limestone, eggshells, shells, or bones. This study synthesized HAp from blood clam shells (*Anadara granosa*) with a CaCO_3 content of 97–99%. Clams are marine biota that lives in mud or on the sand of the ocean. Indonesian people consume blood clams shells as culinary food and handicrafts. The

processing of blood clam shell waste is limited, so the clams shell waste is increasing and accumulating. Based on previous research, the blood clams shells have the main content of CaCO_3 as a source of calcium oxide. The results of Insani et al.'s research [7] stated that the CaO content in blood clams shells was 98%, and the phase with an intensity of 26° and crystal size of 7.79 nm.

HAp as a bone implant material still has several weaknesses, namely its low mechanical properties. According to Ryabenkova et al. [8], an essential condition for a material to be substituted for bone is its ability to bind to living bone or its host in the body. Therefore, to adjust its properties such as biocompatibility, mechanics, and solubility to control the composition, as well as the morphology, organic changes were carried out such as the use of organic compounds in bone implants, one of the methods carried out in this study was the synthesis of HAp composites with polyethylene glycol (PEG) [9]. HAp binds directly through the natural bone conversation mechanism so that it can accelerate bone formation on the implantation surface, but it is fragile. Then it needs to be compiled with biopolymers such as PEG, which is a biocompatible flexible, hydrophilic polymer, nontoxic, and has high tenacity and toughness [10]. In addition, PEG also has corrosion resistance and good chemical and thermal stability. However, PEG also has the disadvantage of having low thermal conductivity. For this reason, the synthesis of HAp-PEG composite is expected to increase the advantages of PEG and HAp so that a composite is formed with the ability as a suitable bone implant material and can be applied in the medical world.

Previous research found that using PEG as a composite material with HAp significantly affected particle size; the particle size of HAp decreased with increasing concentration of PEG in the composite. In addition, it was also found that there was a higher absorption rate than with the use of HAp alone. The temperature of the synthesis also influences the use of PEG as a composite with HAp because the nature of PEG is volatile, and when heated, it hardens quickly. Still, at room temperature, it becomes soft again [11-12]. This paper reports that HAp-PEG composite with a concentration of 70 wt.% has more optimum results in

terms of degradation ability compared to other concentrations, has a hexagonal structure and a crystal size of 24.194 nm, and had needle-shaped crystals, indicating the presence of HAp and agglomerated PEG crystals.

■ EXPERIMENTAL SECTION

Materials

The materials used in this study were blood clam shells collected from the beach, ammonium hydroxide NH_4OH (Merck), diammonium hydrogen phosphate NH_2HPO_4 (Merck), nitric acid HNO_3 p.a (Merck), PEG 6000, Phosphate-buffered saline (PBS, pH = 7.4), filter paper, and aquadest.

Instrumentation

The tools used in this research are mortar, pestle, grinder (Fritsch Pulveristte 16), furnace (Thermo Insight), hot plate, analytical balance, aluminum foil, oven (Labtech), pH indicator, and the necessary laboratory glassware. The characterization tools used are FTIR (FTIR Spectrometer Frontier PerkinElmer), XRD (PANalytical X'Pert PRO), DTA (Shimadzu dtg-60 & Shimadzu ta-60), and SEM EDX (Thermofisher Quatro S).

Procedure

Preparation of CaO powder

The blood clam shells (1.6 g) were cleaned, washed, dried, and ground using a grinder. The mashed blood clam shells were then calcined for 5 h at 900°C to obtain CaO powder [13].

HAp synthesis using sol-gel method

A total of 4.2 g of CaO powder was dissolved in 75 mL of 2 M HNO_3 , then stirred using a stirrer at a temperature of 65°C for 15 min at a speed of 250 rpm; the $\text{Ca}(\text{NO}_3)_2$ solution formed was then filtered. The $\text{Ca}(\text{NO}_3)_2$ filtrate was added with NH_4OH solution until pH 10 was obtained and sol of $\text{Ca}(\text{OH})_2$ was formed. The $\text{Ca}(\text{OH})_2$ sol that has been received is then added drop by drop, a 250 mL solution of 0.18 M $(\text{NH}_4)_2\text{HPO}_4$, then heated at 60°C while stirring using a stirrer for 5 h to form a HAp sol. The HAp sol was then aged for 24 h to

create a gel. The HAp gel was then filtered, then dried using an oven for 5 h at 110 °C [4].

Synthesis of HAp-PEG in-situ

A total of 4 g of PEG was dissolved in 15 mL of distilled water and stirred using a stirrer. In a separate container, 1.6 g of CaO is dissolved in 28 mL of 2 M HNO₃; check the pH of the solution. The dissolved CaO is then added to the PEG solution and stirred using a stirrer until homogeneous. After being homogeneous, this solution was added to the PEG solution while still being mixed, and then checked the pH and added NH₄OH to pH 10. A total of 2.2583 g (NH₄)₂HPO₄ is dissolved with NH₄OH and then mixed; the homogeneous solution is added dropwise into the previous solution then, check the pH of the solution and adjust the pH to pH 10 by adding NH₄OH. After all, were dissolved, they were heated using an oven at a temperature of 60 °C for 24 h. Heating using an oven at a temperature of 60°C because if it is more than 60 °C, it will cause damage to the HAp-PEG composite product that has been formed. The same thing was done for variations in the concentration of HAp on this HAp-PEG composite, with variations in concentrations of 40, 50, 60, 70, and 80% [11,14].

Preparation PBS solution pH 7.4

As much as 8 g of NaCl, 2.38 g of NH₂HPO₄, and 0.19 g of KH₂PO₄ were dissolved in distilled water until the volume is 1 L, then the pH of the solution was measured using a pH meter, and 0.1 M NaOH was added into the solution so that the pH reaches 7.4 [12,15].

Characterization

The product was characterized using an FTIR tool to identify the functional groups of the synthesized composite with measurements in the wave number range of 400–4000 cm⁻¹. XRD tool to determine the structure and crystal size of the synthesized HAp-PEG composite. SEM-EDS tool to determine the surface morphology and determine the Ca/P ratio in the resulting product. DTA tool to determine weight changes in composites related to changes in combustion temperature. The degradation test was carried out by immersing the product in a PBS solution for 14 d, and the product was weighed once every 2 d periodically within that period [16].

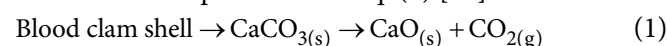
RESULTS AND DISCUSSION

Effect of HAp Concentration on HAp-PEG Composites

Effect synthesis of the HAp-PEG composite was carried out with various concentrations of 40, 50, 60, 70, and 80%, so there were some differences in the resulting product as seen in Table 1. The resulting product is generally white in the form of plates before being heated. The product in the form of a white gel indicates that HAp has been formed in the composite.

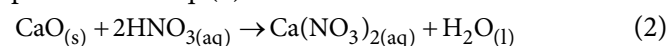
Preparation of CaO from *Anadara granosa*

HAp (Ca₁₀(PO₄)₆(OH)₂) was synthesized from *A. granosa*, because of the high CaCO₃ content, which was as much as 98.7%. CaCO₃ contained in this *A. granosa* is the primary source of calcium in the synthesis of HAp. The cleaned and mashed *A. granosa* were then calcined at 900 °C for 5 h. This calcination process aims to remove organic compounds and reduce CaCO₃ compounds; during this calcination process, a decomposition reaction also occurs, where CaCO₃ become CaO as presented in Eq. (1) [17].

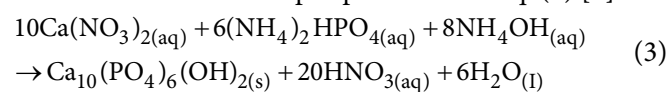


Analysis of HAp Synthesis Results and HAp-PEG Composites

HAp was synthesized using the sol-gel method. The calcined CaO was dissolved with HNO₃ to precipitate unnecessary compounds and form nitrate salts. The solution is then stirred until homogeneous so that unnecessary metals can be dissolved; the reaction is presented in Eq. (2).













Then NH₄OH was added to the Ca(NO₃)₂ solution to form a Ca(OH)₂ sol with a pH of 10; pH 10 is the optimum pH for HAp formation. Sol Ca(OH)₂ then added a solution of (NH₄)₂HPO₄ to form a white gel. The reaction for the formation of HAp is presented in Eq. (3) [8].



The HAp-PEG composite was synthesized with several variations of the concentration of HAp as a matrix

Table 1. Effect of HAp concentration on HAp-PEG composite with various concentrations of 40, 50, 60, 70, and 80%

Concentration variation	Observation before heating	Picture	Observation after heating	Mass (g)	Picture
40%	Gel form and white		Formed a solid that breaks easily but is soft, and there are few cracks	15.4732	
50%	Gel form and white		A solid is formed which breaks easily, and there are more cracks on the composite surface	16.9764	
60%	Gel form and white		Formed solids that break easily, dry, and quite hard	18.8505	
70%	Gel form and white		Formed a solid that breaks easily, dry there are many cracks on the surface, but hard	19.5421	
80%	Gel form and white		Formed solids break easily, dry, and have many cracks on the surface	19.7893	

on PEG. Concentration variations used were 40, 50, 60, 70, and 80%, chosen to see the HAp concentration's effect on the composite formed with the addition of PEG. The analysis showed that the variation of the concentration of HAp 70 wt.% on the HAp-PEG composite showed optimum results [10].

HAp-PEG Composite FTIR Analysis

The results of the FTIR analysis of the HAp-PEG composite for various concentrations of HAp 40, 50, 60, 70, and 80%, as well as pure PEG, are shown in Fig. 1. Fig. 1 shows the FTIR spectrum analysis in the wave range 400–4000 cm^{-1} . Based on the FTIR spectrum results, the absorption occurs at wavenumbers 1027, 1030, 1031, and 1032 cm^{-1} at each concentration (40, 50, 60, 70, and 80%) which indicates the presence of phosphate vibration. In addition, apatite carbonate also showed absorption at wavenumbers of 1430 and 1433 cm^{-1} . FTIR analysis showed that there were characteristics of typical absorption of HAp, namely phosphate, carbonate, and -OH, which were

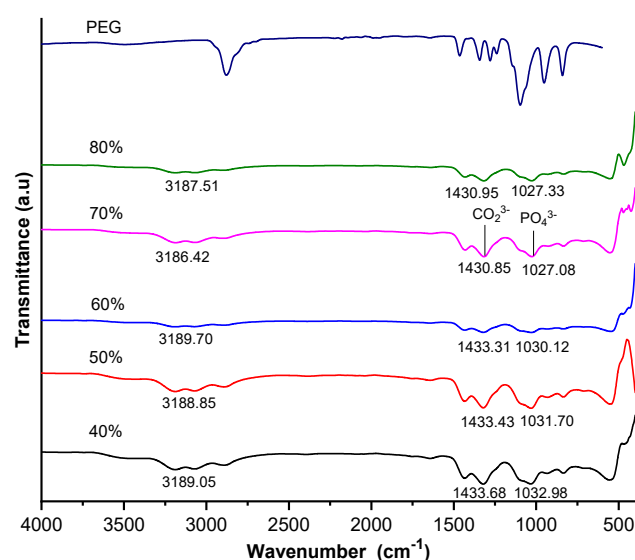


Fig 1. FTIR Spectrum of HAp-PEG composite with various concentrations of 40, 50, 60, 70, and 80 wt.% and PEG 6000

formed by marked PO_4 and PO_3 vibrational peaks from PO_4^{3-} , the appearance of CO vibrational peaks from CO_2

and the presence of -OH absorption bands [3,8,11].

HAp-PEG Composite X-Ray Analysis

The results of the X-ray analysis on the HAp-PEG composite with a concentration of 70 wt.% are shown in Fig. 2. Fig. 2 shows the diffraction pattern of HAp; the diffraction pattern of HAp formed follows the diffraction standard of HAp (ICSD #97849). XRD results prove the presence of HAp in the HAp-PEG composite. In addition to the diffraction pattern of HAp, this X-ray analysis also shows the diffraction pattern of PEG; this is due to the formation of HAp-PEG composite so that the crystallinity of PEG decreases [18].

Scherrer's calculations can determine the crystal size of the formed HAp-PEG composite.

$$L = \frac{k\lambda}{\beta \cos\theta} \quad (4)$$

With the description, L is the crystal size (nm); k is a constant (0.9); λ is the X-ray wavelength; β is FWHM (Full Width at Half Maximum) at 2θ (ϕ 180); θ_B is the Bragg angle [7,19]. Based on the Scherrer equation, it is known that the crystal size of HAp in 70% HAp-PEG composite is 24.194 nm.

HAp-PEG Composite SEM-EDS Analysis

The results of the surface morphology analysis of the HAp-PEG composite with a concentration of 70% magnification of 40,000 \times are shown in Fig. 4. Fig. 4 shows the surface morphology of the HAp-PEG composite with needle-shaped crystals, indicating HAp

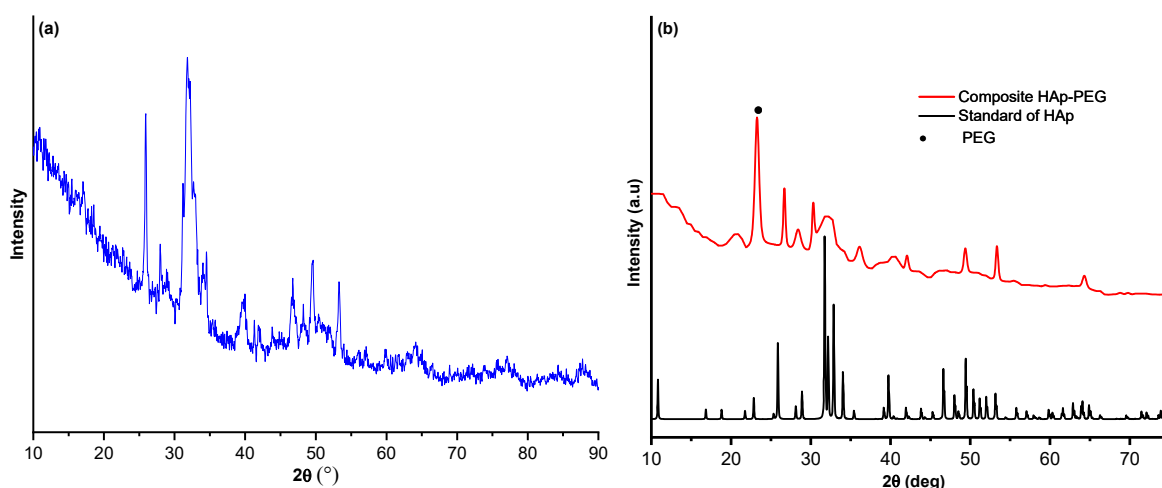


Fig 2. (a) X-ray diffraction of HAp. (b) X-ray diffraction pattern of HAp-PEG composite with a concentration of 70 wt.%

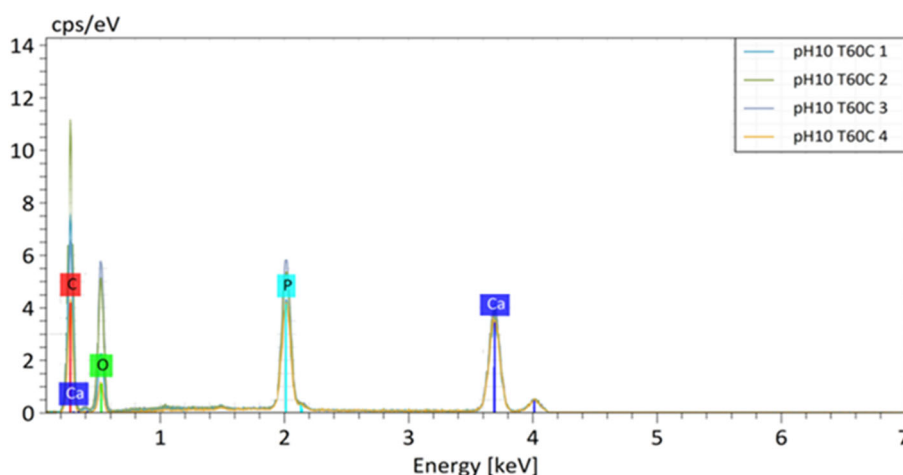


Fig 3. Composition of 70 wt.% HAp-PEG composite through EDS analysis

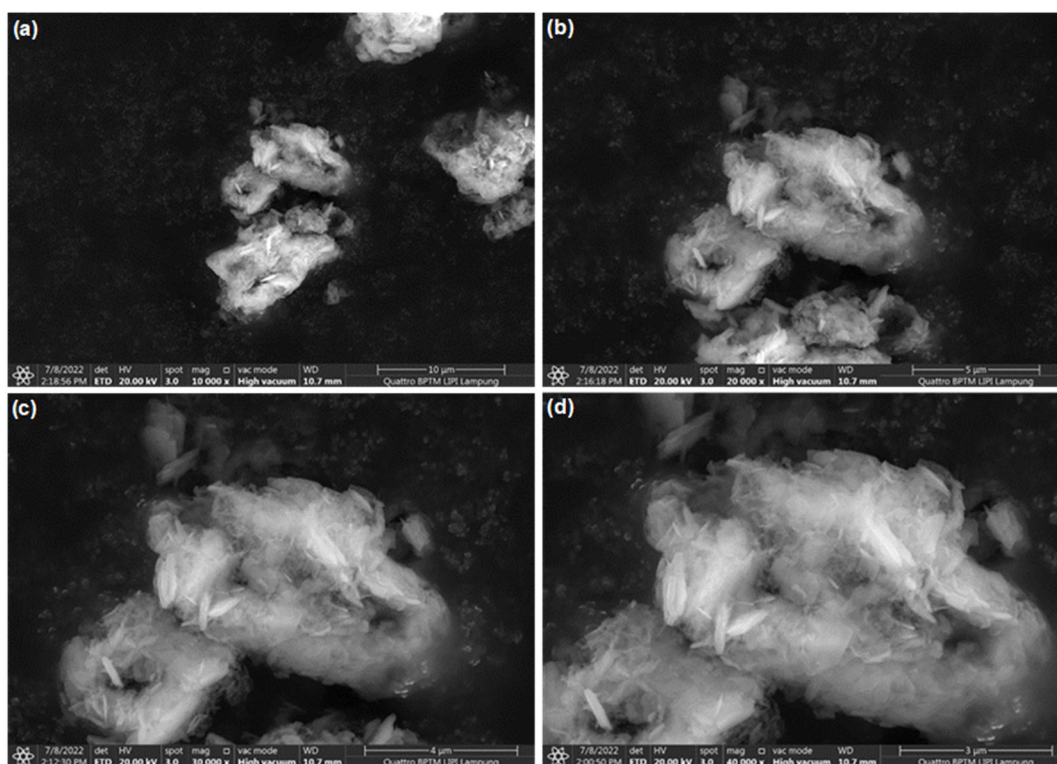


Fig 4. Surface morphology of 70 wt.% HAp-PEG composite on SEM characterization (a) 10,000× magnification (b) 20,000× magnification (c) 30,000× magnification (d) 40,000× magnification

crystals with particles size 5.1 nm. The results shown related to the morphology of the HAp-PEG composite can be influenced by the temperature when carrying out the reaction and the temperature during drying, pH, and the concentration of HAp and PEG in the composite.

To determine the Ca/P Ratio in HAp-PEG composites through SEM-EDS measurements. The composition of the compound in the HAp-PEG composite can be seen in Fig. 3. The compounds contained are C, O, Ca, and P, with the Ca/P ratio value obtained through the EDS measurement of 1.87. The value of the Ca/P ratio obtained is greater than the theoretical Ca/P ratio of 1.67; this indicates that more calcium phosphate is formed than pure Hap [7,19-21].

TGA-DTA Analysis of HAp-PEG Composites

The Hap-PEG composite 70% was analyzed using TGA-DTA at a temperature of 0–900 °C, which can be seen in Fig. 5. The results of the TGA-DTA analysis shown in the temperature range of 50–100 °C resulted in a mass reduction of 8.52% accompanied by an

endothermic reaction as shown in Fig. 5 shown on the DTA chart. Then at a temperature of 200–340 °C, a significant mass reduction occurred as much as 65.72% and was indicated by an exothermic reaction in a very sharp DTA pattern. The reaction is thought to occur due to the decomposition of organic compounds PEG used in the study. While at a temperature of 340–400 °C, a mass

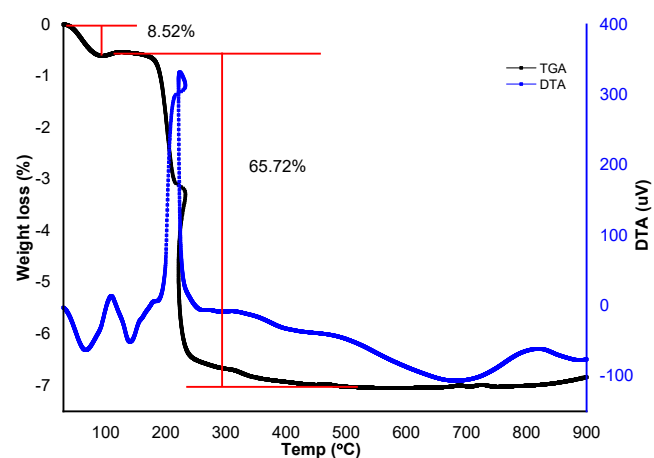


Fig 5. Results of TGA/DTA analysis of HAp-PEG composite 70% at a temperature of 0–900 °C

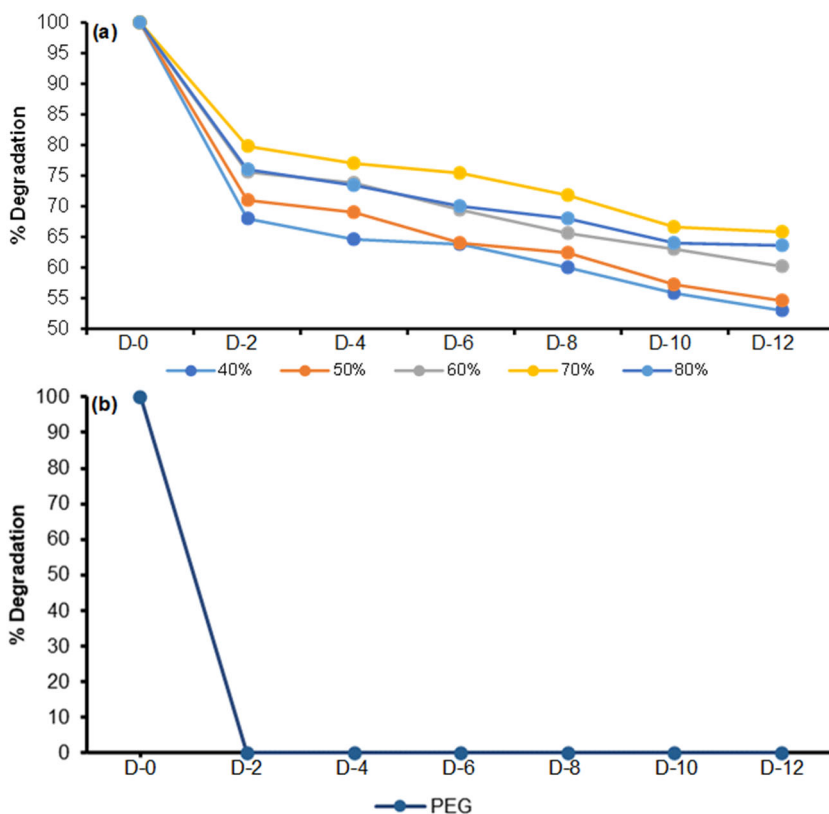


Fig 6. Percent degradation of (a) HAp-PEG composites and (b) PEG with increasing days

reduction is not as significant as 0.31%, accompanied by an endothermic reaction. At temperatures over 400 °C, no mass loss was identified, resulting in a total mass reduction of 74.55% [22-23].

Degradation Test

The ability to form HAp-PEG composite composition on bone was evaluated by immersing it in SBF solution for 14 d. This test can be seen in Fig. 6. Fig. 6 shows a graph of the percent degradation of the HAp-PEG composite. The X-axis shows the degradation testtime of 14 d and is weighed every 2 d, and the Y-axis is the percent degradation. The degradation graph shows the highest proportion of degradation values on the second day, where the weight reduction was significant and on the following day, there was a decrease in weight, and the degradation values slowly then remained constant on the 10th day. The percentage of weight loss in the composite is in line with the increase in PEG. This is in line with the faster degradation test on PEG, as shown in Fig. 6. This indicates that PEG, which is degraded first on

the surface of the HAp-PEG and HAP composites, helps inhibit degradation [24-25]. The interface is a space for water and solvent. High concentrations of HAP will cause an increase in the interface and degradation values.

Measurement of the percentage of degradation of the HAp-PEG composite can be determined by following the following equation:

$$D(\%) = \frac{W_d}{W_0} \times 100\% \quad (5)$$

with the explanation that W_0 and W_d are the percentages of combined weight before and after degradation [9,15].

CONCLUSION

The research results concluded that the HAp composite from blood clam shells (*Anadara granosa*) with PEG had been successfully synthesized using the *in situ* method. HAp-PEG Composite with a concentration of 70 wt.% has more optimum results in terms of degradation ability compared to other concentrations; this is seen from the results of the FTIR measurements

that have been obtained. HAp-PEG Composite 70 wt.% has a hexagonal structure and a crystal size of 24.194 nm according to ICSD #97849 standard. SEM-EDX characterization showed that the HAp-PEG composite sample had needle-shaped crystals, indicating the presence of HAp and agglomerated PEG crystals. The TGA/DTA analysis results showed a weight loss of 65.72% HAp-PEG composite at a temperature higher than 200 °C. The use of PEG for HAp composites also affects the mechanical properties of HAp, such as reduced brittleness, less fracture resistance and a denser structure, meanwhile, if HAp is disturbed it tends to be brittle and easily broken. Still, it does not entirely change the characteristics of HAp, the modification with PEG influenced the physical properties and water adsorption. HAp composites with PEG have the potential to be used as biomedical implant materials.

■ ACKNOWLEDGMENTS

This research was financially supported by the Ministry of Education, Culture, Research, and Technology of the Republic of Indonesia (*Direktorat Jenderal Pendidikan Tinggi, Kementerian Pendidikan dan Kebudayaan Indonesia*) through the national competitive grant [Grant number 086/E5/PG.02.00.PT/2022].

■ AUTHOR CONTRIBUTIONS

Novesar Jamarun collected the experimental data, Vivi Sisca and Nabiila Ayyu Trycahyani drafted the manuscript, and Novesar Jamarun, Syukri Arief, and Upita Septiani developed the idea and corrected the manuscript. All authors read and approved the final manuscript.

■ REFERENCES

- [1] Zhao, C., Liu, W., Zhu, M., Wu, C., and Zhu Y., 2022, Bioceramic-based scaffolds with antibacterial function for bone tissue engineering, *Bioact. Mater.*, 18, 383–398
- [2] Arjunan, A., Baroutaji, A., Praveen, A.S., Robinson, J., and Wang, C., 2020, "Classification of Biomaterial Functionality" in *Encyclopedia of Smart Materials*, Volume 1, Eds. Olabi, A.G., Elsevier, Oxford, 86–102.
- [3] You, B.C., Meng, C.E., Mohd Nasir, N.F., Mohd Tarmizi, E.Z., Fhan, K.S., Kheng, E.S., Abdul Majid, M.S., and Mohd Jamir, M.R., 2022, Dielectric and biodegradation properties of biodegradable nano-hydroxyapatite/starch bone scaffold, *J. Mater. Res. Technol.*, 18, 3215–3226.
- [4] Siregar, A., Jamarun, N., Sisca, V., Yulia Eka, P., 2020, Hydroxiapatites modification with magnesium using calcium from blood blood skin (*Tegillarca granosa*) and test of antibiacy activity, *Rev. Educ.*, 388 (4), 66–73.
- [5] Abere, D.V., Ojo, S.A., Oyatogun, G.M., Paredes-Epinosa, M.B., Niluxsshun, M.C.D., and Hakami, A., 2022, Mechanical and morphological characterization of nano-hydroxyapatite (nHA) for bone regranation: A mini review, *Biomed. Eng. Adv.*, 4, 100056.
- [6] Baladi, M., Amiri, M., Mohammadi, P., Salih Mahdi, K., Golshani, Z., Razavi, R., Salavati-Niazari, M., 2023, Green sol-gel synthesis of hydroxyapatite nanoparticles using lemon extract as capping agent and investigation of its anticancer activity against human cancer cell lines (T98, and SHSY5), *Arabian J. Chem.*, 16 (4), 104646.
- [7] Insani, P.M., and Rahmatsyah, R., 2021, Analysis of the structural pattern of Calcium Carbonate (CaCO₃) on the shells of blood clams (*Anadara granosa*) in Bukit Kerang, Aceh Tamiang Regency, *JTAF*, 9 (1), 23–32.
- [8] Ryabenkova, R., Pinnock, A., Quadros, R.A., Goodchild, R.L., Möbus, G., Crawford, A., Hatton, P.V., and Miller, C.A., 2017, The relationship between particle morphology and rheological properties in injectable nano-hydroxyapatite bone graft substitutes, *Mater. Sci. Eng., C*, 75, 1083–1090.
- [9] Oladele, I.O., Agbabiaka, O.G., Adediran, A.A., Akinwekomi, A.D., and Balogun, A.O., 2019, Structural performance of poultry eggshell derived hydroxyapatite based high density polyethylene bio-composites, *Heliyon*, 5 (10), e02552.
- [10] Abdian, N., Etminanfar, M., Sheykholeslami, S.O.R., Hamishehkar, H., and Khalil-Allafi, J., 2023, Preparation and characterization of

- chitosan/hydroxyapatite scaffolds containing mesoporous SiO₂-HA for drug delivery application, *Mater. Chem. Phys.*, 301, 127672.
- [11] Moeini, S., Mohammadi, M.R., and Simchi, A., 2017, *In-situ* solvothermal processing of polycaprolactone/hydroxyapatite nanocomposites with enhanced mechanical and biological performance for bone tissue engineering, *Bioact. Mater.*, 2 (3), 146–155.
- [12] Chaturvedi, S., Ayaz, S., and Shah, K., 2021, Validated UV spectrophotometric method for *in-vitro* dissolution studies in phosphate buffer pH 7.4, *Int. J. Pharm. Sci. Res.*, 12 (4), 2417–2421.
- [13] Azis, Y., Jamarun, N., Arief, S., and Nur, H., 2015, Facile synthesis of hydroxyapatite particles from cockle shells (*Anadara granosa*) by hydrothermal method, *Orient. J. Chem.*, 31 (2), 1099–1105.
- [14] Monte, J.P., Fontes, A., Santos B.S., and Pereira, G.A.L., 2023, Recent advances in hydroxyapatite/polymer/silver nanoparticles scaffolds with antimicrobial activity for bone regeneration, *Mater. Lett.*, 338, 134027.
- [15] Frasnelli, M., Cristofaro, F., Sglavo, V.M., Dirè, S., Callone, E., Ceccato, R., Bruni, G., Cornaglia, A.I., and Visai, L., 2017, Synthesis and characterization of strontium-substituted hydroxyapatite nanoparticles for bone regeneration, *Mater. Sci. Eng., C*, 71, 653–662.
- [16] Jamarun, N., Yuwan, S., Juita, R., and Rahayuningsih, J., 2015, Synthesis and characterization carbonate apatite from bukit Tui limestone Padang Indonesia, *J. Appl. Chem.*, 4 (2), 542–549.
- [17] Zahir, M.H., Rahman, M.M., Irshad, K., and Rahman, M.M., 2019, Shape-stabilized phase change materials for solar energy storage: MgO and Mg(OH)₂ mixed with polyethylene glycol, *Nanomaterials*, 9 (12), 1773.
- [18] Jamarun, N., Azharman, Z., Arief, S., Sari, T.P., Asril, A., and Elfina, S., 2015, Effect of temperature on synthesis of hydroxyapatite from limestone, *Rasayan J. Chem.*, 8 (1), 133–137.
- [19] Trakoolwannachai, V., Kheolamai, P., and Ummartyotin, S., 2019, Characterization of hydroxyapatite from eggshell waste and polycaprolactone (PCL) composite for scaffold material, *Composites, Part B*, 173, 106974.
- [20] Talaei, H., Fallah-Mehrjardi, M., and Hakimi, F., 2018, Polyethylene glycol-(*N*-methylimidazolium) hydroxide-grafted γ -Fe₂O₃@Hap: A novel nanomagnetic recyclable basic phase-transfer catalyst for the synthesis of tetrahydrobenzopyran derivatives in aqueous media, *J. Chin. Chem. Soc.*, 65 (5), 523–530.
- [21] Adamu, D.B., Zereffa, E.A., Segne, T.A., Razali, M.H., and Lemu, B.R., 2023, Synthesis and characterization of bismuth-doped hydroxyapatite nanorode for fluoride removal, *Environ. Adv.*, 12, 100360.
- [22] Jamarun, N., Azharman, Z., and Septiani, U., 2016, Effect of firing for synthesis of hydroxyapatite by precipitation method, *Orient. J. Chem.*, 32 (4), 2095–2099.
- [23] Hartatiek, H., Utomo, J., Noerjannah, L.I., Rohmah, N.Z., and Yudyanto, Y., 2021, Physical and mechanical properties of hydroxyapatite/polyethylene glycol nanocomposites, *Mater. Today: Proc.*, 44, 3263–3267.
- [24] Nurlidar, F., and Kobayashi, M., 2019, Succinylated bacterial cellulose induce carbonated hydroxyapatite deposition in a solution mimicking body fluid, *Indones. J. Chem.*, 19 (4), 858–864.
- [25] Senra, M.R., de Lima, R.B., de Holanda Saboya Souza, D., Marques, M.F.V., and Monteino, S.N., 2020, Thermal characterization of hydroxyapatite or carbonated hydroxyapatite hybrid composites with distinguished collagens for bone graft, *J. Mater. Res. Technol.*, 9 (4), 7190–7200.